Journal of Clinical and Translational Hepatology **2022** vol. 10(4) | 577–588
DOI: 10.14218/JCTH.2021.00289

Original Article

Overexpression of Hepcidin Alleviates Steatohepatitis and Fibrosis in a Diet-induced Nonalcoholic Steatohepatitis

Hui Chen[1*], Wenshan Zhao[2,3], Xuzhen Yan[2,3], Tao Huang[2,3] and Aiting Yang[2,3,4*]

[1]Digestive Department, Beijing Chaoyang Hospital, Capital Medical University, Beijing, China; [2]Experimental and Translational Research Center, Beijing Friendship Hospital, Capital Medical University, Beijing, China; [3]National Clinical Research Center of Digestive Diseases, Beijing, China; [4]Beijing Clinical Medicine Institute, Beijing, China

Received: 17 July 2021 | **Revised:** 22 September 2021 | **Accepted:** 28 September 2021 | **Published:** 4 January 2022

Abstract

Background and Aims: Iron overload can contribute to the progression of nonalcoholic fatty liver disease (NAFLD) to nonalcoholic steatohepatitis (NASH). Hepcidin (Hamp), which is primarily synthesized in hepatocytes, is a key regulator of iron metabolism. However, the role of Hamp in NASH remains unclear. Therefore, we aimed to elucidate the role of Hamp in the pathophysiology of NASH. ***Methods:*** Male mice were fed a choline-deficient L-amino acid-defined (CDAA) diet for 16 weeks to establish the mouse NASH model. A choline-supplemented amino acid-defined (CSAA) diet was used as the control diet. Recombinant adeno-associated virus genome 2 serotype 8 vector expressing Hamp (rAAV2/8-Hamp) or its negative control (rAAV2/8-NC) was administered intravenously at week 8 of either the CDAA or CSAA diet. ***Results:*** rAAV2/8-Hamp treatment markedly decreased liver weight and improved hepatic steatosis in the CDAA-fed mice, accompanied by changes in lipogenesis-related genes and adiponectin expression. Compared with the control group, rAAV2/8-Hamp therapy attenuated liver damage, with mice exhibiting reduced histological NAFLD inflammation and fibrosis, as well as lower levels of liver enzymes. Moreover, α-smooth muscle actin-positive activated hepatic stellate cells (HSCs) and CD68-postive macrophages increased in number in the CDAA-fed mice, which was reversed by rAAV2/8-Hamp treatment. Consistent with the *in vivo* findings, overexpression of Hamp increased adiponectin expression in hepatocytes and Hamp treatment inhibited HSC activation. ***Conclusions:*** Overexpression of Hamp using rAAV2/8-Hamp robustly attenuated liver steatohepatitis, inflammation, and fibrosis in an animal model of NASH, suggesting a potential therapeutic role for Hamp.

Citation of this article: Chen H, Zhao W, Yan X, Huang T, Yang A. Overexpression of Hepcidin Alleviates Steatohepatitis and Fibrosis in a Diet-induced Nonalcoholic Steatohepatitis. J Clin Transl Hepatol 2022;10(4):577–588. doi: 10.14218/JCTH.2021.00289.

Introduction

Nonalcoholic fatty liver disease (NAFLD) is one of the most prevalent liver diseases worldwide. Hepatic manifestation of metabolic syndrome associated with NAFLD is highly prevalent in obese and diabetic inidividuals.[1,2] Nonalcoholic steatohepatitis (NASH) is a subtype of NAFLD that can progress to cirrhosis, liver failure, hepatocellular carcinoma, and death. Despite the severe outcomes of NASH, there are no known efficacious treatments for NASH-related advanced fibrosis. Thus, there is an urgent need to develop new therapies.[3–5]

The pathogenesis of liver inflammation and fibrosis in patients with NAFLD is not completely understood. Other than insulin resistance, iron overload has been considered an indicator of inflammation and fibrosis. Accumulating evidence suggests that approximately one-third of USA and Chinese patients with biopsy-proven NAFLD develop hepatic iron stores.[6–8] Increased iron stores could be of pathogenic importance in NAFLD, since elevated iron levels can increase the risk of hepatocyte ballooning, inflammation, and fibrosis, all of which are characteristics of NASH. Iron reduction therapy could potentially reduce steatosis and insulin resistance, as well as serum transaminase activity in patients with NASH/NAFLD.[9–11] However, treatment of iron overload presents some challenges. A meta-analysis showed that iron depletion does not significantly improve indices of insulin resistance, liver enzyme levels, or liver histology compared to lifestyle changes alone in patients with NAFLD.[12]

Hepcidin (Hamp) is an acute-phase reactant produced primarily in the liver, that was first identified as an antimicrobial peptide and was subsequently shown to play a central role in regulating iron homeostasis. There is increasing evidence to suggest that its synthesis is regulated in response to inflammation, hypoxia, and iron homeostasis.[13,14] Taking this into account, the increased Hamp levels in NAFLD are most likely induced by elevated inflammatory cytokines; therefore, there has been great interest in evaluating Hamp as a potential non-invasive biomarker of NAFLD. Of note, serum Hamp levels have previously been reported to be

Keywords: Liver fibrosis; Hepatic stellate cell; Hepcidin; NASH; CDAA.

Abbreviations: ALT, alanine aminotransferase; AST, aspartate aminotransferase; CDAA, choline-deficient L-amino acid-defined; CSAA, choline-supplemented amino acid-defined; Hb, Hemoglobin; HSCs, hepatic stellate cells; NAFLD, nonalcoholic fatty liver disease; NASH, nonalcoholic steatohepatitis; rAAV, recombinant adeno-associated virus.

***Correspondence to:** Hui Chen, Digestive Department, Beijing Chaoyang Hospital, Capital Medical University, No. 5 Jingyuan Road, Shijingshan District, Beijing 100043, China. Tel: +86-10-51718484, Fax: +86-10-83165944, E-mail: chenhui_0516@126.com. Aiting Yang, Experimental and Translational Research Center, Beijing Friendship Hospital, Capital Medical University, No. 95 Yong'an Road, Xicheng District, Beijing 100050, China. ORCID: https://orcid.org/0000-0002-5671-696X. Tel: +86-10-63139311, Fax: +86-10-83165944, E-mail: yangaiting168@126.com

correlated with obesity but not liver disease.[15–17] Despite the fact that the mechanism through which Hamp induces NAFLD remains uncertain, excessive cytokines, such as interleukin (IL) 6, have a core function in Hamp production. More interestingly, Tsutsumi *et al.*[18] recently found that there was a significant inverse correlation between Hamp immunoreactivity and fibrosis in pediatric NAFLD patients, suggesting that these patients experienced a reduction in the Hamp-producing ability of the liver in response to iron levels, leading to subsequent fibrosis.

Our preliminary data also demonstrated that low levels of Hamp are associated with murine carbon tetrachloride (CCl_4)-induced liver fibrosis, leading to the hypothesis that Hamp might be effective in treating NASH-related fibrosis. Therefore, we sought to determine if Hamp contributes to the severity of steatosis, inflammation, and fibrosis in a mouse model of NASH induced by a choline-deficient l-amino acid-defined (CDAA) diet. We used a recombinant adeno-associated virus genome 2 serotype 8 (rAAV2/8) vector to efficiently transfect a Hamp overexpressing plasmid into liver cells to investigate the effects of Hamp on NASH-related inflammation and fibrosis in a mouse model.

Methods

Experimental animals

This study was approved by the Institutional Animal Care and Usage Committee of the Beijing Friendship Hospital, Capital Medical University. C57BL/6J mice were fed a CDAA diet (M10530i; Moldiets Co. Ltd., Chengdu, China) for 16 weeks to induce NASH. The control group received a CSAA diet (M10530Ci; Moldiets). Recombinant adeno-associated virus subtype 2/8 vector expressing Hamp (rAAV2/8-Hamp) or its negative control vector (rAAV2/8-NC) were amplified by Obio (Shanghai, China). Mice were treated with either the rAAV2/8-NC or rAAV2/8-Hamp via tail vein injection at a dose of 3×10^{11} genome copies/mouse after 8 weeks of being fed either the CDAA or CSAA diet. The mice were housed on a 12 h light/dark cycle, with controlled temperature (23±2°C) at 40–60% humidity.

Food intake and body weight were monitored weekly. After a total of 16 weeks on the CDAA or CSAA diet, animals were euthanized and sacrificed. Serum was collected and frozen, and the livers and spleens were dissected, weighed, and snap-frozen for further analysis.

Hamp treatment

The rat hepatic stellate cell (HSC) line-T6 was a gift from Dr. Scott Friedman (Mount Sinai Medical Center, New York, NY, USA). T6 cells were plated in Dulbecco's modified Eagle medium (DMEM) supplemented with 10% (v/v) fetal bovine serum (FBS). When cells reached 80–90% confluence, they were detached using trypsin and reseeded at 2×10^5 per well in a 6-well plate. T6 cells were cultured overnight in serum-free medium before experimentation. Cells were stimulated with Hamp (10 ng/mL or 100 ng/mL; Peptide Institute, Osaka, Japan) and cultured for 48 h. Control cells were left unstimulated.

Generation of Hamp-overexpressing hepatocyte cell line

AML12 mouse hepatocytes (American Type Culture Collection, Manassas, VA, USA) were cultured in DMEM/F12 with 10% FBS supplemented with 1% Insulin-Transferrin-Selenium (ITS) (51500056; Invitrogen, Waltham, MA, USA), 40 ng/mL dexamethasone, and 1% penicillin streptomycin mixture. The plRES2-EGFP-NC and plRES2-EGFP-Hamp plasmids were transfected into AML12 cells using the EndoFectin™ Max transfection reagent (GeneCopoeia, Rockville, MD, USA) following the manufacturer's instructions. Briefly, AML12 cells (5×10^4 per well) were seeded into a 12-well plate. After 24 h, the cells were transfected with either 2 or 4 μg of the plasmids using the EndoFectin™ Max transfection reagent.

Quantitative real-time (q)PCR analysis

Total mRNA was extracted using the TRIzol reagent (Sigma-Aldrich, St. Louis, MO, USA) according to the manufacturer's protocol.[19] Reverse transcription was performed with 1 μg total RNA using the SuperScript™ VILO™ Master Mix (Invitrogen). The SYBR Green Real-time PCR Master Mix (Invitrogen) was used for qPCR. Primers used for qPCR are listed in Table 1. Glyceraldehyde-3-phosphate dehydrogenase (GAPDH) was used to normalize the PCR results, and the ΔΔCt method was used for quantification.

Western blot analysis

Total cell lysates were homogenized in tissue lysis buffer (FNN0071; Invitrogen) supplemented with protease and phosphatase inhibitors (Roche, Basel, Switzerland).[20] Proteins were resolved by SDS-PAGE and transferred to nitrocellulose membranes (Amersham Biosciences, Buckinghamshire, UK). Membranes were then incubated with primary antibodies against alpha-smooth muscle actin (αSMA) (diluted 1:500; Abcam, Cambridge, UK), tissue inhibitor of metalloproteinase (TIMP)1 (diluted 1:500; Invitrogen), and β-actin (diluted 1:2,000; Peprotech, Rocky Hill, NJ, USA) overnight at 4°C. On the following day, the membranes were incubated with the appropriate secondary antibodies (Cell Signaling Technology, Danvers, MA, USA) and proteins were visualized using a chemiluminescent substrate (Invitrogen).

Histopathological analysis

Liver samples were fixed with neutral-buffered formalin, embedded in paraffin, and cut into 4-μm thick sections that were stained with either hematoxylin and eosin (HE) or Sirius Red (SR), or prepared for immunohistochemistry (IHC) analysis of αSMA and CD68 expression.

Histological assessment and scoring were performed by a pathologist blinded to the study. Steatosis and lobular inflammation scoring on liver histology were performed using the clinical criteria outlined by Kleiner *et al*.[21] Activated HSCs and total macrophages were detected using an anti-αSMA antibody (diluted 1:200; Abcam) and an anti-CD68 antibody (diluted 1:500; Invitrogen), respectively. Morphometric quantification of SR staining (percentage of area) was performed at 200× in 10 random fields per mouse from five individual animals using ImageJ software. αSMA- and CD68-positive cells were quantified as the number of positively stained cells per high-power field (HPF).

For Oil-red O staining, optimal cutting temperature-embedded frozen tissue was sectioned at 7 μm and fixed in 10% neutral buffered formalin. After washing with distilled water, dried slides were subsequently incubated with 60% isopropanol and Oil-red O solution, then rinsed with 60% isopropanol solution and distilled water and mounted with glycerin. Morphometric quantification of Oil-red O staining (percentage of area) was performed at 200× in 10 random fields per

Table 1. Primers used for qPCR

Gene	Primer sequences	Product size	Accession No
Hamp	F: 5′-CAATGTCTGCCCTGCTTTCT-3′	113 bp	NM_032541.2
	R: 5′-TCTCCTGCTTCTCCTCCTTG-3′		
αSMA	F: 5′-GATGAAGCCCAGAGCAAGAG-3′	87 bp	XM_021152572.1
	R: 5′-CTTTTCCATGTCGTCCCAGT-3′		
COL1A1	F: 5′-GAGCGGAGAGTACTGGATCG-3′	158 bp	NM_007742.4
	R: 5′-GCTTCTTTTCCTTGGGGTTC-3′		
CCR2	F: 5′-GGCTCAGCCAGATGCAGTTAA-3′	76 bp	NM_011333.3
	R: 5′-CCTACTCATTGGGATCATCTTGCT -3′		
TGFβ-1	F: 5′-GAGGTCACCCGCGTGCTA-3′	70 bp	NM_011577.2
	R: 5′-TGTGTGAGATGTCTTTGGTTTTCTC-3′		
Il10	F: 5′-GCTCTTACTGACTGGCATGAG-3′	105 bp	NM_010548.2
	R: 5′-CGCAGCTCTAGGAGCATGTG-3′		
TNFα	F: 5′-TCCCAGGTTCTCTTCAAGGGA-3′	51 bp	NM_001278601.1
	R: 5′-GGTGAGGAGCACGTAGTCGG-3′		
TIMP-1	F: 5′-CCAGAGCCGTCACTTTGCTT-3′	126 bp	NM_001294280.2
	R: 5′-AGGAAAAGTAGACAGTGTTCAGGCTT -3′		
SREBP1c	F: 5′-TGGAGACATCGCAAACAAG-3′	274 bp	XM_030245748.1
	R: 5′-GGTAGACAACAGCCGCATC-3′		
ChREBP	F: 5′-AGATGGAGAACCGACGTATCA-3′	104 bp	NM_001359237.1
	R: 5′-ACTGAGCGTGCTGACAAGTC-3′		
Acc	F: 5′-GATGAACCATCTCCGTTGGC-3′	65 bp	XM_030245463.1
	R: 5′-GACCCAATTATGAATCGGGAGTG-3′		
Scd1	F: 5′-TGACCTGAAAGCCGAGAA-3′	342 bp	NM_009127.4
	R: 5′-ATGTGCCAGCGGTACTCA-3′		
Adiponectin	F: 5′-TGTTCCTCTTAATCCTGCCCA-3′	104 bp	NM_009605.5
	R: 5′-CCAACCTGCACAAGTTCCCTT-3′		
GAPDH	F: 5′-TCCACTCACGGCAAATTCAAC-3′	89 bp	XM_017321385.1
	R: 5′-CGCTCCTGGAAGATGGTGATG-3′		

αSMA, smooth muscle alpha-actin; COL1A1, collagen type I alpha 1 chain; CCR2, C-C motif chemokine receptor 2; TGFβ-1, transforming growth factor-beta 1; Il10, interleukin 10; TNF, tumor necrosis factor; TIMP-1, tissue inhibitor of metalloproteinase 1; SREBP1c, sterol-regulatory element binding protein-1c; ChREBP, carbohydrate response element binding protein; Acc, acetyl coenzyme A carboxylase; Scd1, steatoyl-coenzyme A desaturase 1; GAPDH, glyceraldehyde 3-phosphate dehydrogenase.

mouse from five individual animals using ImageJ software.

Serum biochemistry

Serum samples were stored at −80°C until analyses could be performed. Serum aspartate aminotransferase (AST), alanine aminotransferase (ALT), and iron were measured using Olympus Beckman Coulter AU480 automatic biochemistry analysis system reagents (InTec Products, Shenzhen, China) provided by the manufacturer. Hemoglobin (Hb) levels were measured using the Mindray Bc 3000 Automatic Blood Cell Analyzer according to the manufacturer's recommendations.

Statistical analysis

Data were expressed as mean±standard error of the mean (SEM) and were analyzed using GraphPad Prism software (v.5; GraphPad Software, La Jolla, CA, USA). A Student's *t*-test was used to compare values obtained from two groups. Data from multiple groups were compared using a one-way ANOVA followed by the Tukey's post-hoc test. Finally, *p*-values <0.05 were considered significant.

Results

rAAV2/8-Hamp treatment increased Hamp expression in CDAA-induced NASH

To investigate the anti-steatotic effects of Hamp, we fed mice a CDAA diet for 16 weeks, which is commonly used to induce steatosis in mouse models of NASH. The mice were administered a total dose of 3×10^{11} genome copies per mouse of either rAAV2/8-Hamp or rAAV2/8-NC after 8 weeks of either

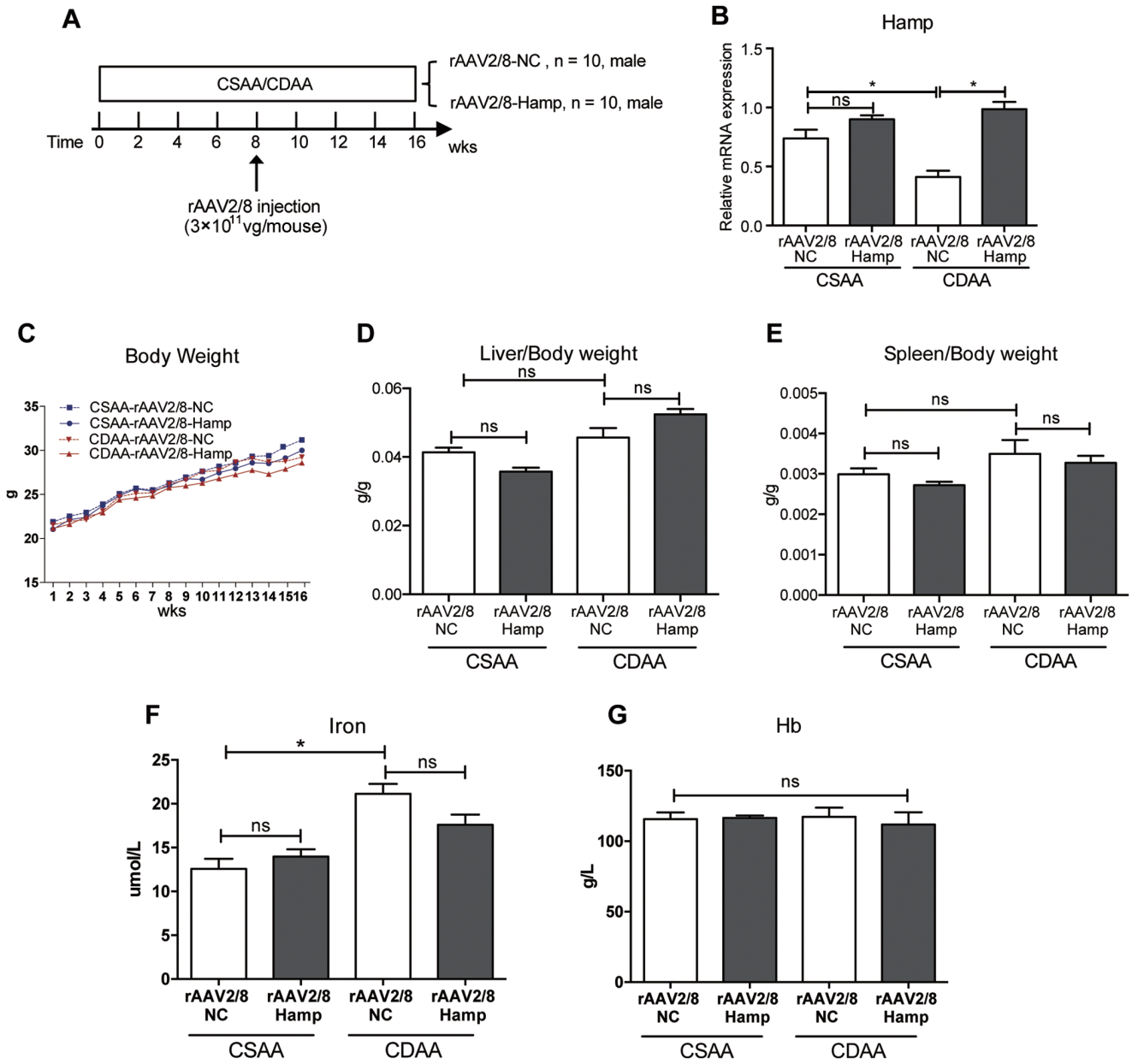

Fig. 1. Hamp levels increased following rAAV2/8-Hamp treatment in mice fed CDAA or CSAA diets for 16 weeks. (A) Male mice (8 weeks-old) were fed either the CSAA or CDAA diet for 16 weeks with rAAV2/8-NC or rAAV2/8-Hamp treatment at week 8 (n=10 per group). (B) Hamp gene expression, (C) growth curve, (D) relative liver mass, (E) relative spleen mass, (F) serum iron levels, and (G) Hb levels in mice fed either the CSAA or CDAA diet for 16 weeks. Data represent the mean±SEM of at least 10 animals per group. CDAA, choline-deficient L-amino acid-defined; CSAA, choline-supplemented amino acid-defined; rAAV, recombinant adeno-associated virus; NC, negative control; Hb, Hemoglobin.

the CDAA or control CSAA diet (Fig. 1A). We found that Hamp mRNA levels were significantly lower in the CDAA-fed mice compared to the CSAA-fed mice, as expected. We also found that Hamp was increased in all liver tissues from mice injected with rAAV2/8-Hamp compared to rAAV2/8-NC (Fig. 1B).

rAAV2/8-Hamp treatment reduced body weight gain without affecting iron status and Hb levels

Both the CSAA and CDAA diets have been shown to cause a progressive and time-dependent increase in body weight. In our model, the CDAA-fed mice gained less body weight (~6% less) compared to the CSAA-fed mice after 16 weeks. It is worth noting that rAAV2/8-Hamp treatment decreased body weight gain in the control group (~5% lower) (Fig. 1C). Food intake (data not shown) following rAAV2/8-Hamp and rAAV2/8-NC treatment in both the CDAA- and CSAA-fed mice increased at similar rates and there were no differences in relative liver weight and spleen weight between the two groups (Fig. 1D–E).

Hamp is a master regulator of systemic iron homeostasis, and therefore tightly controls erythrocyte production. We measured serum iron and Hb levels among the four

groups of mice. Serum iron levels were significantly higher in the CDAA-fed mice compared to the CSAA-fed mice, but rAAV2/8-Hamp treatment did not significantly decrease serum iron levels compared to rAAV2/8-NC treatment in either the CDAA- or CSAA-fed mice (Fig. 1F). Hb levels were similar among the four groups (Fig. 1G). Our data suggest that overexpression of Hamp in liver tissue does not induce systemic iron overload or affect Hb levels.

rAAV2/8-Hamp treatment reversed steatosis in CDAA-fed mice

We next determined whether increased Hamp expression following rAAV2/8-Hamp transduction reversed CDAA-induced hepatic steatosis. HE staining showed evidence of hepatic steatosis (primarily as micro- and macro-steatosis) in the CDAA-fed mice, and rAAV2/8-Hamp treatment remarkably decreased the hepatic lipid deposition in the CDAA-fed mice compared to the rAAV2/8-NC treatment (Fig. 2A). The semi-quantitative steatosis data were confirmed using lipid morphometry on Oil-red O stained liver sections; we observed an approximate three-fold decrease in the rAAV2/8-Hamp treatment group compared to the rAAV2/8-NC treatment group of the CDAA-fed mice (54.34±6.14% vs. 18.91±2.42%, respectively; $p<0.05$) (Fig. 2B). In addition, the steatosis score was lower in the rAAV2/8-Hamp treatment group compared to the rAAV2/8-NC treatment group (2.80±0.42 vs. 1.70±0.67, respectively; $p<0.05$) (Fig. 2C).

The CSAA-fed mice group showed significant glucose intolerance compared to that of the CDAA-fed mice group after a 16-week feeding. rAAV2/8-Hamp treatment significantly improved oral glucose tolerance at 60, 90, and 120 m after gavage with glucose in the CSAA group; however, there was no difference between rAAV2/8-Hamp and rAAV2/8-NC administration in the CDAA group. These results indicate that Hamp effectively attenuated CSAA-induced changes in metabolic parameters (Fig. 2D).

rAAV2/8-Hamp treatment modulates the expression of lipogenesis-related genes

To further explore the underlying mechanisms of steatohepatitis, we determined the difference in lipid metabolism following rAAV2/8-Hamp treatment in both the CDAA- and CSAA-fed mice. Compared to the CSAA diet, the CDAA diet significantly down-regulated the expression of genes involved in *de novo* lipogenesis. These genes included carbohydrate response element binding protein (ChREBP), sterol regulatory binding protein 1c (SREBP1c), Stearoyl-CoA desaturase 1 (Scd1), acetyl-CoA carboxylase (Acc), and adiponectin. rAAV2/8-Hamp treatment down-regulated, although not significantly, the expression of these lipogenesis-related genes in the CSAA-fed mice. In contrast, rAAV2/8-Hamp treatment significantly up-regulated the expression of ChREBP and SREBP1c in the CDAA-fed mice but had no effect on the expression of Scd1 and Acc1 between the two groups (Fig. 3E–H). Interestingly, rAAV2/8-Hamp treatment increased adiponectin expression in the CDAA-fed mice compared to the rAAV2/8-NC treatment (Fig. 3I).

Hamp overexpression modulated adiponectin expression in AML12 cells

To further evaluate the role of Hamp in hepatocyte adiponectin expression, we transfected mouse hepatocyte AML12 cells with either the plRES2-Hamp or plRES2-NC plasmid (Fig. 3A). Consistent with the *in vivo* study, we found that expression of adiponectin was dramatically elevated in the AML12 cells transfected with plRES2-Hamp compared to plRES2-NC (Fig. 3B–C).

rAAV2/8-Hamp treatment suppressed liver inflammation in CDAA-fed mice

We next analyzed liver inflammation in the CDAA- and CSAA-fed mice treated with rAAV2/8-Hamp after 16 weeks. Immunostaining analysis of CD68, a well-established marker of activated macrophages, showed that CD68 expression was significantly increased in the CDAA-fed mice compared to the CSAA-fed mice. Treatment with rAAV2/8-Hamp significantly attenuated CDAA-induced macrophage infiltration and decreased the inflammation score (Fig. 4A–C).

Aspartate aminotransferase (AST) and alanine aminotransferase (ALT) activity significantly increased in the CDAA-fed mice compared to the CSAA-fed mice. Treatment with rAAV2/8-Hamp in the CDAA-fed mice significantly decreased the serum ALT and AST levels compared to the rAAV2/8-NC treatment (Fig. 4D–E).

In line with these findings, livers from the CDAA-fed mice had increased mRNA levels of chemokine (C-C motif) receptor 2 (CCR2) and tumor necrosis factor alpha (TNFα) compared to the CSAA-fed mice, whereas expression of these genes was suppressed in CDAA-fed mice treated with rAAV2/8-Hamp (Fig. 4F–G). The mRNA levels of Il10, a potent anti-inflammatory cytokine, were significantly higher in the livers of the CDAA-fed mice compared to the CSAA-fed mice, and expression of Il10 was slightly increased in the CDAA-fed mice treated with rAAV2/8-Hamp (Fig. 4H).

rAAV2/8-Hamp treatment ameliorated liver fibrosis in CDAA-fed mice

Finally, we evaluated liver fibrosis in the CDAA- and CSAA-fed mice treated with rAAV2/8-Hamp after 16 weeks. Collagen deposition and HSC activation were significantly increased in the CDAA-fed mice compared to the CSAA-fed mice, and rAAV2/8-Hamp treatment reduced these fibrosis markers in the CDAA-fed mice, as assessed by SR staining and IHC detection of αSMA (Fig. 5A–C). Similarly, livers from CDAA-fed mice had increased mRNA levels of COL1A1, αSMA, and TIMP-1 compared to CSAA-fed mice, and rAAV2/8-Hamp treatment suppressed expression of these genes in the CDAA-fed mice (Fig. 5D–F).

Hamp supplementation showed anti-fibrotic effects in HSCs in vitro

Considering the major pathophysiological role that HSCs have in fibrogenesis, we investigated the effect of Hamp in cultured HSC T6 cells. Specifically, we measured the expression of fibrogenetic genes (αSMA, TIMP-1, COL1A1, and transforming growth factor beta 1 [TGFβ-1]). Hamp (10 and 100 ng/mL) dose-dependently and significantly reduced the mRNA levels of fibrogenetic genes after 48 h of incubation compared to unstimulated HSCs (Fig. 6A–D). Reduction of αSMA and TIMP1 were also confirmed at the protein level, as determined by quantitative western blot analysis (Fig. 6E).

Discussion

Iron-load is prevalent in a third of NAFLD patients and can

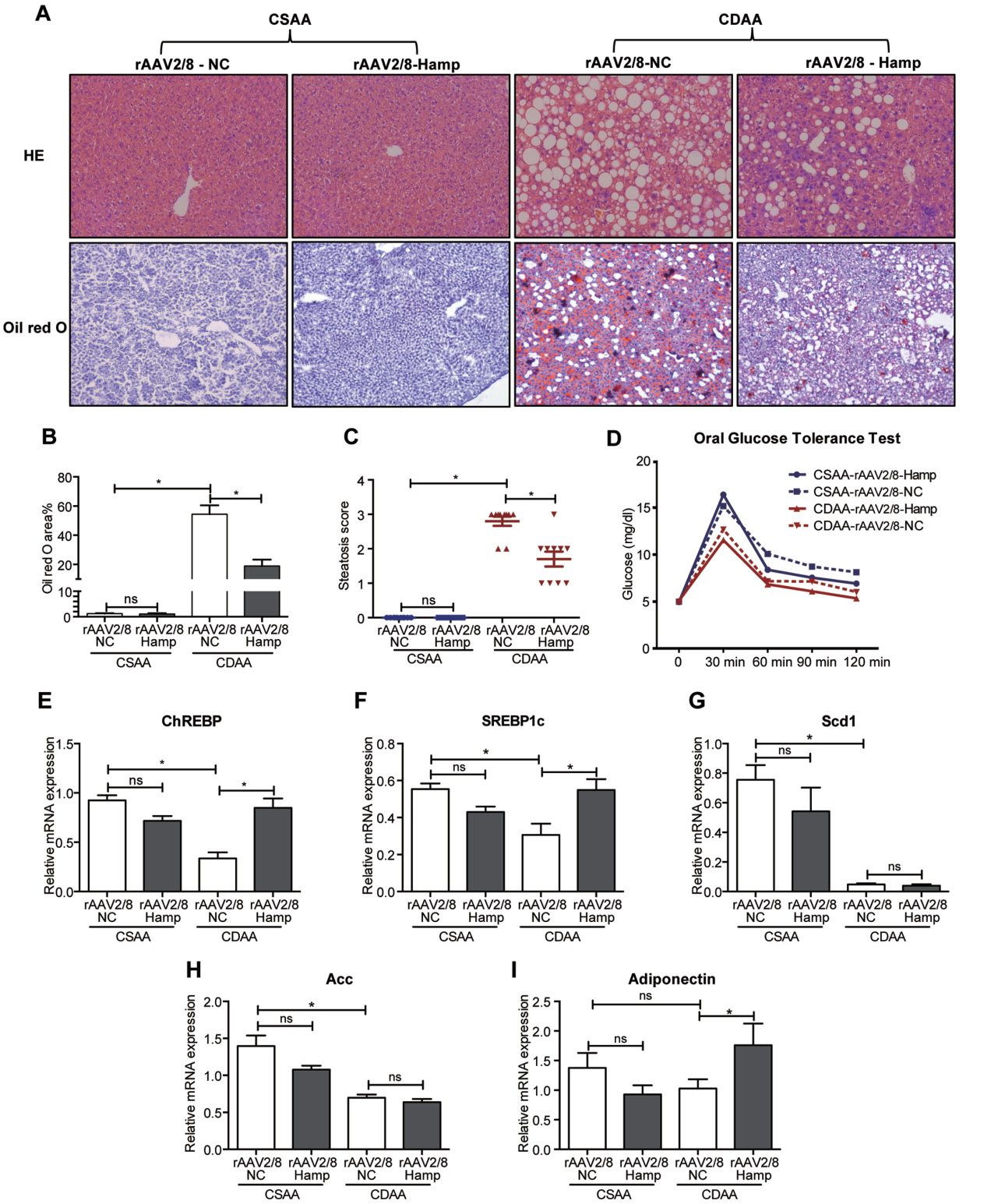

Fig. 2. rAAV2/8-Hamp treatment showed anti-steatotic properties in CDAA-fed mice. (A) Representative HE (original magnification 200×) and Oil-red O staining images (original magnification 100×) in liver sections of mice treated with rAAV2/8-Hamp or rAAV2/8-NC for up to 16 weeks. (B) Quantification of Oil-red O staining images of mice fed either the CDAA or CSAA diet. (C) Liver steatosis scores. (D) Oral glucose tolerance test. (E–I) Hepatic transcript levels of ChREBP, SREBP1c, Scd1, Acc, and adiponectin in mice fed either the CDAA or CSAA diet for 16 weeks. Data represent the mean±SEM of at least 10 animals per group. HE, hematoxylin-eosin; CDAA, choline-deficient L-amino acid-defined; CSAA, choline-supplemented amino acid-defined; rAAV, recombinant adeno-associated virus; ChREBP, carbohydrate response element binding protein; SREBP1c, sterol-regulatory element binding protein-1c; Scd1, steatoyl-coenzyme A desaturase 1; Acc, acetyl coenzyme A carboxylase.

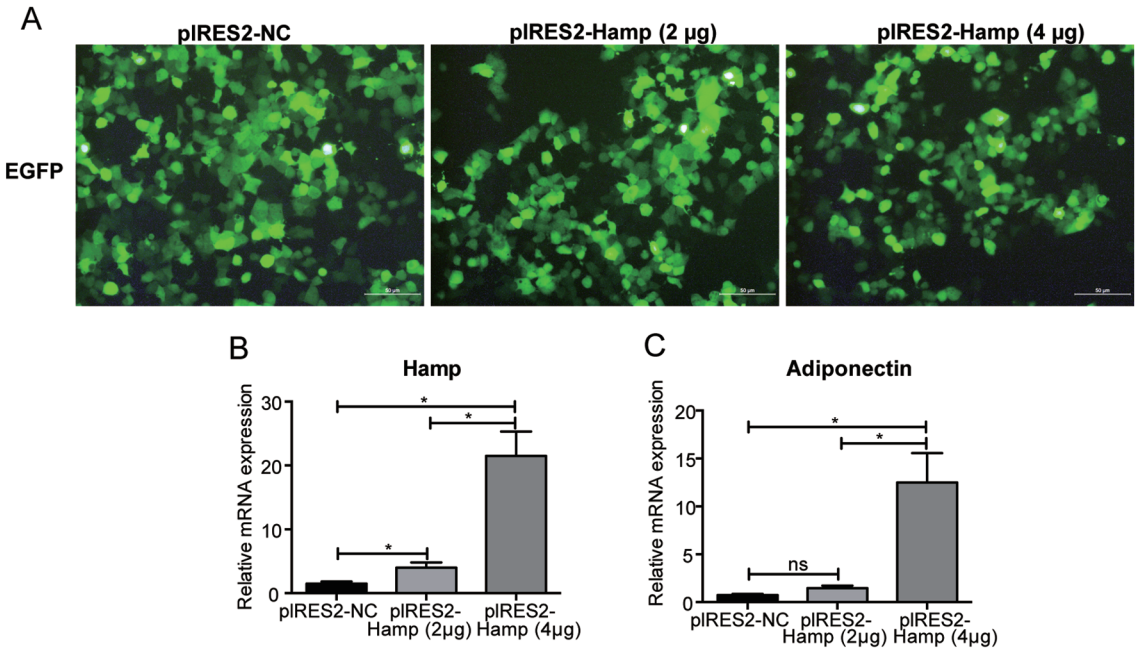

Fig. 3. Hamp overexpression modulated adiponectin expression in AML12 cells. AML12 hepatocytes were transduced with either the Hamp overexpression plasmid or the NC plasmid. (A) Transfection efficiency was visualized using fluorescence microscopy. (B, C) Transcript levels of Hamp and adiponectin. Data represent the mean±SEM. NC, negative control.

accelerate the progression of steatosis, fibrosis, cirrhosis, and hepatocellular carcinoma. As such, iron removal therapy has become a potential treatment strategy for NASH.[6,7] Given its role in regulating iron homeostasis, Hamp has gained attention as a promising therapeutic agent that can remove liver iron stores.[13,14] In the present study, our data showed that rAAV2/8-Hamp treatment significantly suppressed CDAA diet-induced steatosis, hepatic inflammation, and subsequent liver fibrosis in mice.

A choline-deficient diet can increase the onset of steatohepatitis features and fibrosis in mice, similar to patients with rapid NASH progression. Since our main focus is understanding how to best treat NASH-related fibrosis, we established the CDAA mouse model to best mirror pathology and pathogenesis of human NASH. In agreement with previous studies, the CDAA diet resulted in moderate hepatic lipoapoptosis, liver inflammation, and fibrosis, while the CSAA diet led to severe insulin resistance and absence of inflammation and fibrosis.[22–24] Mice on the CDAA developed macrovesicular steatosis in the liver, but the CDAA-fed mice developed a metabolic profile opposite to what is observed in human disease. We found that the CDAA diet significantly down-regulated the expression of genes involved in fatty acid synthesis, which might result from compensatory hepatic uptake of serum lipids or by impairment in very low-density lipoprotein secretion from the liver. NAFLD in patients has a complex and heterogeneous pathogenesis, thus it should be pointed out that animal models of NAFLD may not recapitulate all characteristics of human disease.

In our study, we first found that Hamp expression was significantly down-regulated and that iron stores were increased in the CDAA-fed mice, suggesting an important role for Hamp in the pathogenesis of NASH. Hamp is mostly produced by hepatocytes in response to iron loading in cells. As iron loads increase, Hamp expression also increases in hepatocytes, resulting in elevated serum Hamp level.[25] Patients with chronic liver diseases have evidence of liver dysfunction and anemia associated with inflammation but surprisingly also have lower serum Hamp levels compared to control subjects.[26] Similar findings have been reported in alcoholic chronic liver diseases,[27] chronic hepatitis C,[28,29] hepatitis B virus-related cirrhosis,[30–33] and in autoimmune liver diseases.[34] Hamp levels in NAFLD are difficult to interpret, since Hamp expression is likely to be regulated by complex mechanisms in response to diverse pathophysiological stimuli. In the later stages of NAFLD/NASH, serum Hamp levels are not suppressed, and the levels eventually decrease in NAFLD with advanced fibrosis, similar to other liver diseases.[18]

Although accumulating evidence shows that serum Hamp levels and iron metabolism are related to serum markers of steatosis, inflammation, fibrosis, and insulin resistance, no study has investigated if Hamp supplementation could be used as a therapeutic strategy for NASH. Here, we first investigated the possible effect of rAAV2/8-Hamp on CDAA diet-induced hepatic steatosis in mice. Our data demonstrated that treatment with rAAV2/8 significantly attenuated CDAA diet-induced hepatic steatosis without affecting iron and Hb levels. While the CDAA diet is a well-established nutritional NAFLD model, the metabolic profile of this diet does not completely reflect all properties of NAFLD. Specifically, other aspects of metabolic dysregulation are not necessarily accounted for because hepatic lipid accumulation in the model is mainly due to impaired secretion of very low-density lipoprotein. Our study showed that overexpression of Hamp corrected the abnormal expression of SREBP1c and ChREBP. This could partially explain the mechanism by which rAAV2/8-Hamp treatment can suppress CDAA diet-induced hepatic steatosis and regulate lipid metabolism. Furthermore, we noted that rAAV2/8-Hamp treatment normalized the loss in body weight in the CDAA diet-induced NASH model.

Increased inflammation is a hallmark of NASH. Thus, controlling liver inflammation may be a potential strategy to treat NASH. Macrophages are key cells that induce the release of inflammatory mediators, such as TNFα, CCR2, and

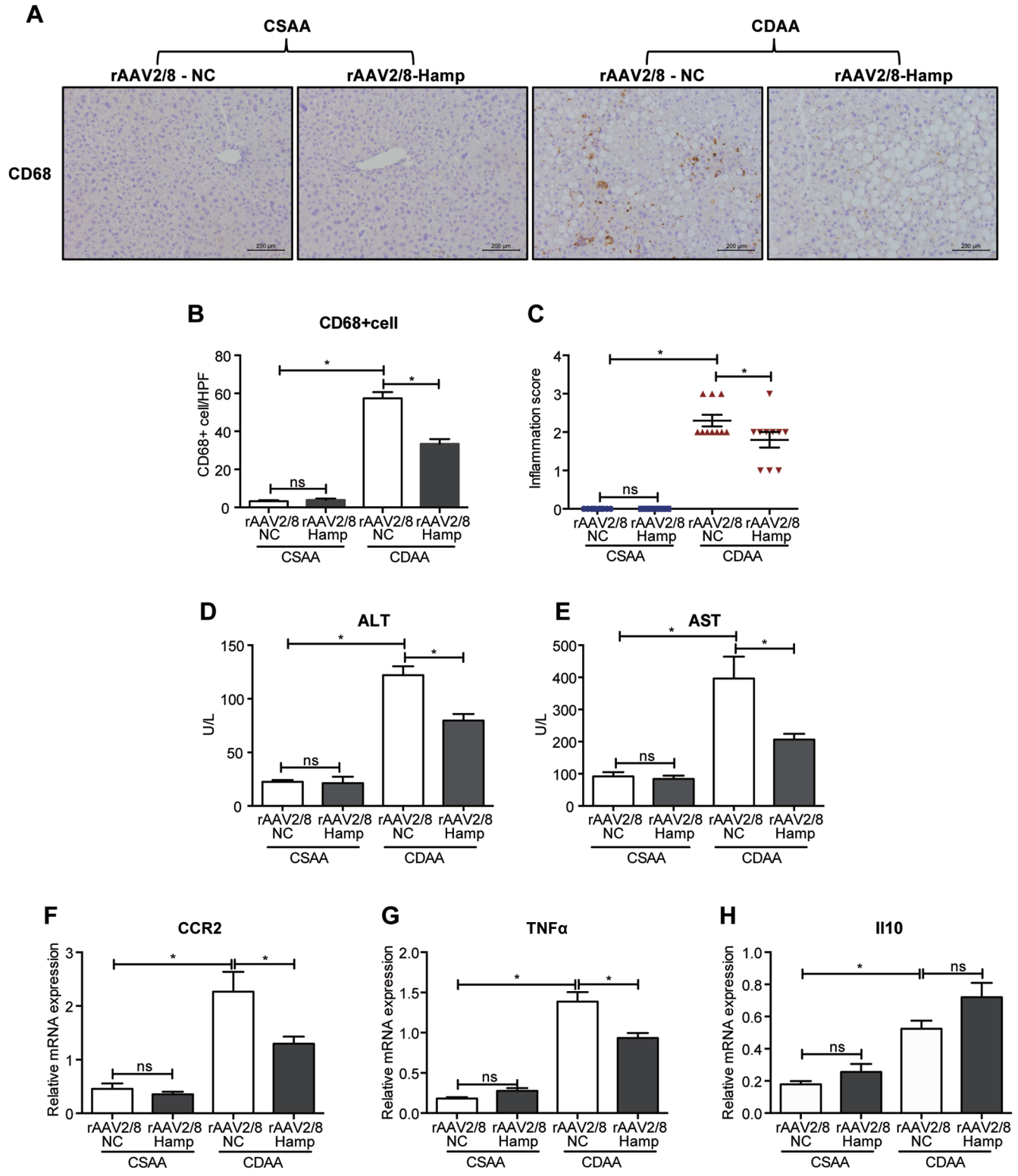

Fig. 4. rAAV2/8-Hamp treatment suppressed hepatic inflammation in CDAA-fed mice. (A) Representative CD68-positive macrophages (original magnification 200×) in liver sections of mice treated with rAAV2/8-Hamp or rAAV2/8-NC. (B) Quantification of images of mice fed either the CDAA or CSAA diet. rAAV2/8-Hamp treatment decreased (D) serum ALT and (E) AST levels in mice fed a CDAA diet compared with rAAV2/8-NC treatment. (F–H) Transcript levels of CCR2, TNFα and Il10. Data represent the mean±SEM of at least 10 animals per group. CDAA, choline-deficient L-amino acid-defined; CSAA, choline-supplemented amino acid-defined; rAAV, recombinant adeno-associated virus; ALT, alanine aminotransferase; AST, aspartate aminotransferase; NC, negative control; CCR2, C-C Motif chemokine receptor 2; TNF, tumor necrosis factor; Il10, interleukin 10.

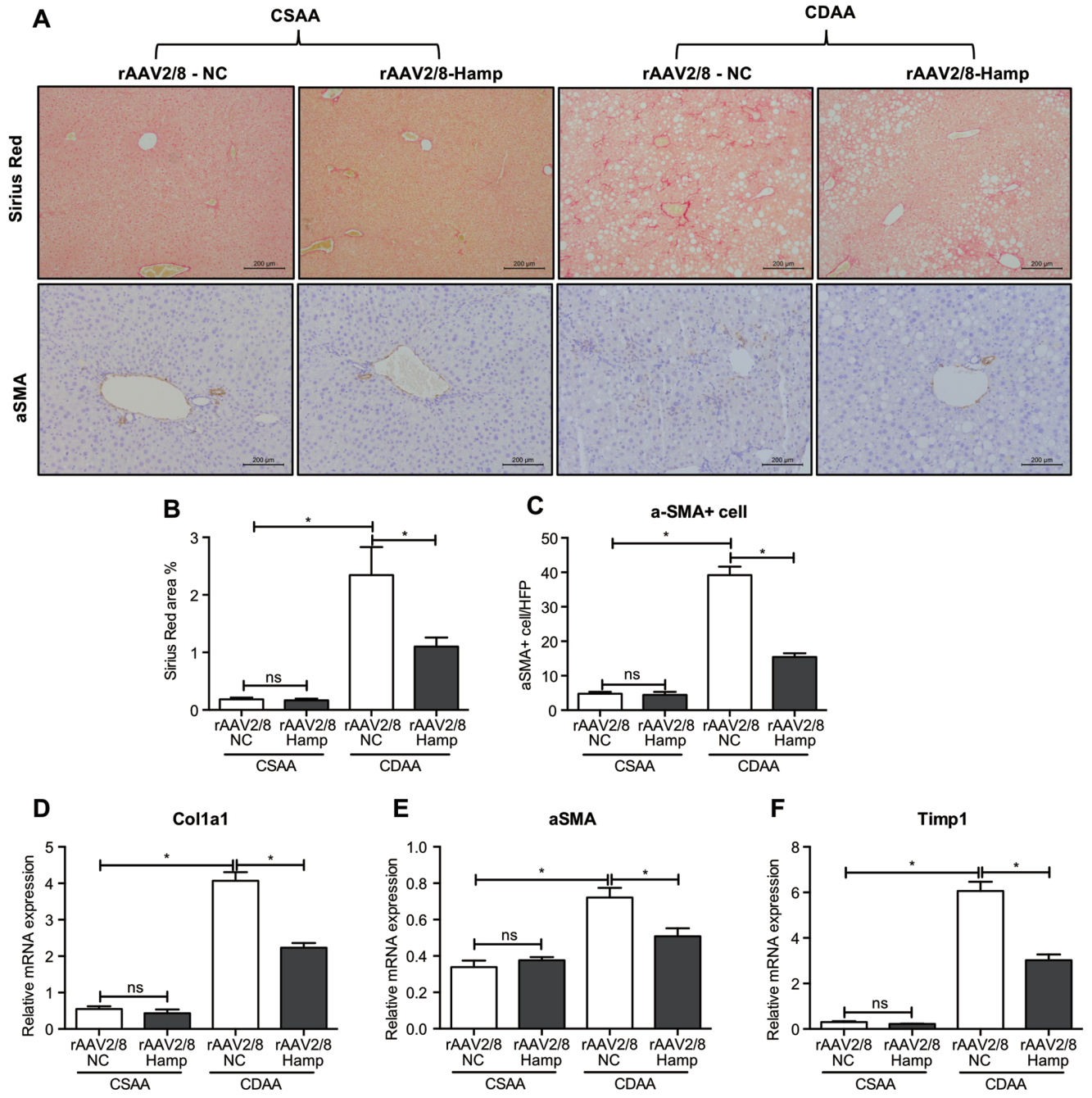

Fig. 5. rAAV2/8-Hamp treatment suppressed hepatic fibrosis in mice fed a CDAA diet. (A) Representative SR staining (top; original magnification 200×) and αSMA-positive HSCs (bottom; original magnification 200×) in liver sections of mice treated with rAAV2/8-Hamp or rAAV2/8-NC. (B–C) Quantification of images of mice fed either the CDAA or CSAA diet. (D–F) Transcript levels of COL1A1, αSMA, and TIMP-1. Data represent the mean±SEM of at least 10 animals per group. SR, sirius red; CDAA, choline-deficient L-amino acid-defined; CSAA, choline-supplemented amino acid-defined; rAAV, recombinant adeno-associated virus; αSMA, smooth muscle alpha-actin; HSCs, hepatic stellate cells; NC, negative control; COL1A1, collagen type I alpha 1 chain; TIMP-1, tissue inhibitor of metalloproteinase 1.

IL1β in NASH.[35–37] These inflammatory mediators further stimulate hepatocytes and HSCs to induce hepatocyte steatosis and fibrosis, respectively. As expected, overexpression of Hamp decreased the CDAA diet-induced levels of hepatic CD68-positive macrophages and altered the inflammatory response in our model, as indicated by a down-regulation in pro-inflammatory cytokines (TNFα and CCR2) and a slight up-regulation in the anti-inflammatory cytokine (IL10).

Hamp expression is controlled mainly at the transcriptional level by various stimuli, including inflammation, iron status, and hypoxia. The link between inflammation/infection and liver production of Hamp is attributed to IL6 produced at the sites of infection/inflammation. IL6 binds to the IL6-receptor and phosphorylates JAK-2/STAT3, which binds to and activates the Hamp promoter.[38] Importantly, Hamp can also influence the function of macrophages. Zla-

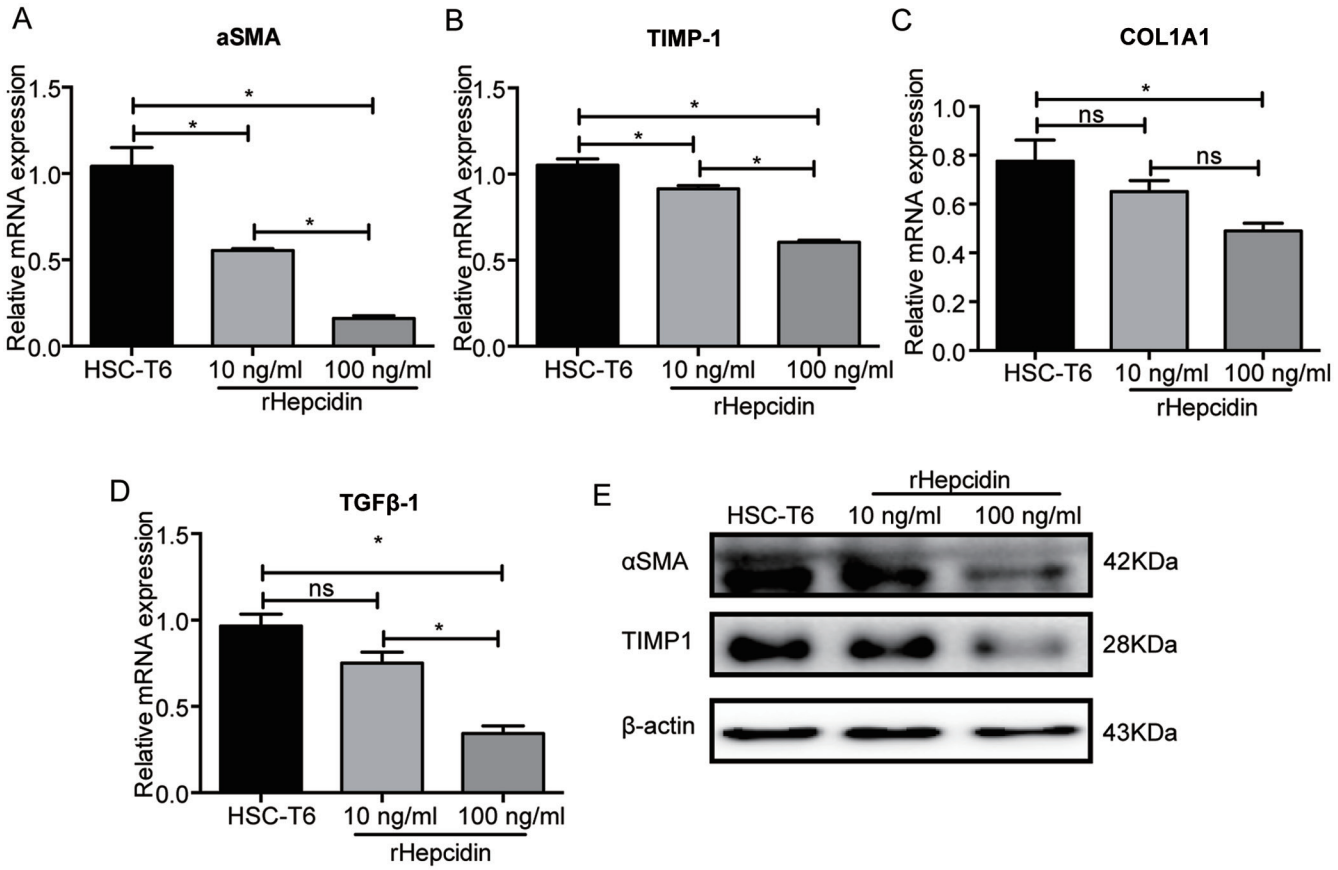

Fig. 6. Effect of hepcidin on HSCs activation. HSCs were stimulated with hepcidin (10 or 100 ng/mL) for 48 h. (A–D) Gene expression of (A) αSMA, (B) TIMP-1, (C) COL1A1, and TGFβ-1 (D) in HSCs. (E) Protein expression of αSMA and TIMP1 in HSCs. Data represent the mean±SEM. HSCs, hepatic stellate cells; αSMA, smooth muscle alpha-actin; TIMP-1, tissue inhibitor of metalloproteinase 1; COL1A1, collagen type I alpha 1 chain; TGFβ-1, transforming growth factor-beta 1.

tanova *et al*.[39] reported that Hamp-induction by IL6 and/or iron could reduce the secretion of IL4 and IL13 in macrophages, thereby inhibiting cardiac repair. In contrast, Hamp-deficiency in macrophages promoted the release of IL4 and IL13 by recombinant IL6. It has been suggested that Hamp is an upstream repressor of reparatory cytokines (IL4 and IL13) secreted by cardiac macrophages. A similar study showed that Hamp induces M1 macrophage polarization.[40] In contrast, another study showed that Hamp reduced M1 polarization of RAW264.7 macrophages. The authors explain that this discrepancy may be caused by factors such as differential simulation, iron concentration, and cell condition.[41] We found that overexpression of Hamp in liver cells decreased the number of CD68-positive macrophages in the liver**.** Moreover, mRNA expression of pro-inflammatory cytokines, such as CCR2 and TNFα, decreased significantly, suggesting a role for Hamp in liver inflammation and macrophage infiltration.

Our study suggests an important role of Hamp in HSC activation, which results in hepatic fibrosis following a CDAA diet. The CDAA diet decreased Hamp expression, which was accompanied by HSC activation, as demonstrated by an increase in αSMA-positive cells. Furthermore, expression of fibrotic genes (αSMA, TIMP-1, and COL1A1) was significantly reduced in the livers of the CDAA-fed mice following rAVV2/8-Hamp treatment. Consistent with our data, pharmacological administration of Hamp has been shown to improve fibrosis by blocking activation of HSCs both in the CCl_4 and bile duct ligation fibrosis models.[42,43] Conversely, when challenged with an iron-overload diet, Hamp knockout mice displayed significant liver fibrosis associated with iron accumulation and stellate cell activation.[44] In liver fibrosis, low Hamp levels cause high iron load and oxidative stress. Oxidative stress and lack of Hamp-induced suppression induces HSC activation, which results in scar tissue deposition and liver fibrosis.[34] Cell-based assays provide a mechanism whereby exogenous Hamp hinders TGFβ1-induced SMAD-3 phosphorylation in HSCs, inhibiting their activation. On the other hand, there have been contradictory reports as to the role of Hamp in NASH/NAFLD. Hamp knockout NAFLD mice develop liver damage. Although loss of Hamp is associated with a reduction in liver steatosis, liver fibrosis is present early and is more pronounced in the knockout mice compared to mice with normal Hamp expression.[45] Different animal models of NASH involve several factors, including various degrees of hepatocyte damage, insulin resistance, inflammation, and lipid metabolism, all of which can affect the regulation of Hamp. Therefore, regulation of Hamp and consequently iron homeostasis need to be further investigated.

It is noteworthy that the beneficial effects of Hamp overexpression on lipid metabolism and inflammation may be due to HSC activation and induced adiponectin expression. Adiponectin is the predominant adipokine made by adipose tissue and is involved in the regulation of hepatic lipid metabolism. In addition to its metabolic effects, growing evidence suggests that adiponectin possesses potent anti-fibrotic and anti-inflammatory properties.[46,47]

Altogether, we demonstrated for the first time that rAAV2/8-Hamp treatment ameliorated CDAA-induced inflammation and related liver fibrosis as well as improved lipid metabolic abnormalities, suggesting that rAAV2/8-mediated Hamp intervention may have beneficial effects on NASH. This increase in hepatic Hamp produced a marked induction of adiponectin both *in vivo* and *in vitro*. Furthermore, Hamp directly inhibited HSC fibrogenesis *in vitro*. To fully understand the protective and therapeutic function of Hamp, other dietary animal models, such as high fat- or western diet-induced NAFLD, should be explored.

Funding

National Natural Science Foundation of China (No. 81900547).

Conflict of interest

The authors have no conflict of interests related to this publication.

Author contributions

Study conception and drafting of the manuscript (HC, AY), and performance of experiments or analysis of the resultant data (HC, WZ, XY, TH, AY). All authors read or revised the manuscript.

Data sharing statement

All data are available upon request.

References

[1] Wong RJ, Aguilar M, Cheung R, Perumpail RB, Harrison SA, Younossi ZM, *et al*. Nonalcoholic steatohepatitis is the second leading etiology of liver disease among adults awaiting liver transplantation in the United States. Gastroenterology 2015;148(3):547–555. doi:10.1053/j.gastro.2014.11.039.
[2] Schuppan D, Surabattula R, Wang XY. Determinants of fibrosis progression and regression in NASH. J Hepatol 2018;68(2):238–250. doi:10.1016/j.jhep.2017.11.012.
[3] Cusi K. A diabetologist's perspective of non-alcoholic steatohepatitis (NASH): Knowledge gaps and future directions. Liver Int 2020;40(Suppl 1):S82–S88. doi:10.1111/liv.14350.
[4] Schuppan D, Schattenberg JM. Non-alcoholic steatohepatitis: pathogenesis and novel therapeutic approaches. J Gastroenterol Hepatol 2013;28(Suppl 1):S68–S76. doi:10.1111/jgh.12212.
[5] Negro F. Natural history of NASH and HCC. Liver Int 2020;40(Suppl 1):S72–S76. doi:10.1111/liv.14362.
[6] Nelson JE, Klintworth H, Kowdley KV. Iron metabolism in Nonalcoholic Fatty Liver Disease. Curr Gastroenterol Rep 2012;14(1):8–16. doi:10.1007/s11894-011-0234-4.
[7] Sachinidis A, Doumas M, Imprialos K, Stavropoulos K, Katsimardou A, Athyros VG. Dysmetabolic Iron Overload in Metabolic Syndrome. Curr Pharm Des 2020;26(10):1019–1024. doi:10.2174/1381612826666200130090703.
[8] Xu J, Sun W, Yang L. Association between iron metabolism and cognitive impairment in older non-alcoholic fatty liver disease individuals: A cross-sectional study in patients from a Chinese center. Medicine (Baltimore) 2019;98(48):e18189. doi:10.1097/MD.0000000000018189.
[9] Abe N, Tsuchida T, Yasuda SI, Oka K. Dietary iron restriction leads to a reduction in hepatic fibrosis in a rat model of non-alcoholic steatohepatitis. Biol Open 2019;8(5):bio040519. doi:10.1242/bio.040519.
[10] Salaye L, Bychkova I, Sink S, Kovalic AJ, Bharadwaj MS, Lorenzo F, *et al*. A Low Iron Diet Protects from Steatohepatitis in a Mouse Model. Nutrients 2019;11(9):2172. doi:10.3390/nu11092172.
[11] Sumida Y, Kanemasa K, Fukumoto K, Yoshida N, Sakai K, Nakashima T, *et al*. Effect of iron reduction by phlebotomy in Japanese patients with non-alcoholic steatohepatitis: A pilot study. Hepatol Res 2006;36(4):315–321. doi:10.1016/j.hepres.2006.08.003.
[12] Murali AR, Gupta A, Brown K. Systematic review and meta-analysis to determine the impact of iron depletion in dysmetabolic iron overload syndrome and non-alcoholic fatty liver disease. Hepatol Res 2018;48(3):E30–E41. doi:10.1111/hepr.12921.
[13] Milic S, Mikolasevic I, Orlic L, Devcic E, Starcevic-Cizmarevic N, Stimac D, *et al*. The Role of Iron and Iron Overload in Chronic Liver Disease. Med Sci Monit 2016;22:2144–2151. doi:10.12659/msm.896494.
[14] Saneela S, Iqbal R, Raza A, Qamar MF. Hepcidin: A key regulator of iron. J Pak Med Assoc 2019;69(8):1170–1175.
[15] Bekri S, Gual P, Anty R, Luciani N, Dahman M, Ramesh B, *et al*. Increased adipose tissue expression of hepcidin in severe obesity is independent from diabetes and NASH. Gastroenterology 2006;131(3):788–796. doi:10.1053/j.gastro.2006.07.007.
[16] Auguet T, Aragonès G, Berlanga A, Martínez S, Sabench F, Binetti J, *et al*. Hepcidin in morbidly obese women with non-alcoholic fatty liver disease. PLoS One 2017;12(10):e0187065. doi:10.1371/journal.pone.0187065.
[17] Marmur J, Beshara S, Eggertsen G, Onelöv L, Albiin N, Danielsson O, *et al*. Hepcidin levels correlate to liver iron content, but not steatohepatitis, in non-alcoholic fatty liver disease. BMC Gastroenterol 2018;18(1):78. doi:10.1186/s12876-018-0804-0.
[18] Tsutsumi N, Nishimata S, Shimura M, Kashiwagi Y, Kawashima H. Hepcidin Levels and Pathological Characteristics in Children with Fatty Liver Disease. Pediatr Gastroenterol Hepatol Nutr 2021;24(3):295–305. doi:10.5223/pghn.2021.24.3.295.
[19] Yang AT, Hu DD, Wang P, Cong M, Liu TH, Zhang D, *et al*. TGF-β1 Induces the Dual Regulation of Hepatic Progenitor Cells with Both Anti- and Proliver Fibrosis. Stem Cells Int 2016;2016(2016):1492694. doi:10.1155/2016/1492694.
[20] Zhao W, Yang A, Chen W, Wang P, Liu T, Cong M, *et al*. Inhibition of lysyl oxidase-like 1 (LOXL1) expression arrests liver fibrosis progression in cirrhosis by reducing elastin crosslinking. Biochim Biophys Acta Mol Basis Dis 2018;1864(4 Pt A):1129–1137. doi:10.1016/j.bbadis.2018.01.019.
[21] Kleiner DE, Brunt EM, Van Natta M, Behling C, Contos MJ, Cummings OW, *et al*. Design and validation of a histological scoring system for nonalcoholic fatty liver disease. Hepatology 2005;41(6):1313–1321. doi:10.1002/hep.20701.
[22] Farrell G, Schattenberg JM, Leclercq I, Yeh MM, Goldin R, Teoh N, *et al*. Mouse Models of Nonalcoholic Steatohepatitis: Toward Optimization of Their Relevance to Human Nonalcoholic Steatohepatitis. Hepatology 2019;69(5):2241–2257. doi:10.1002/hep.30333.
[23] Gore E, Bigaeva E, Oldenburger A, Jansen YJM, Schuppan D, Boersema M, *et al*. Investigating fibrosis and inflammation in an ex vivo NASH murine model. Am J Physiol Gastrointest Liver Physiol 2020;318(2):G336–G351. doi:10.1152/ajpgi.00209.2019.
[24] Wei G, An P, Vaid KA, Nasser I, Huang P, Tan L, *et al*. Comparison of murine steatohepatitis models identifies a dietary intervention with robust fibrosis, ductular reaction, and rapid progression to cirrhosis and cancer. Am J Physiol Gastrointest Liver Physiol 2020;318(1):G174–G188. doi:10.1152/ajpgi.00041.2019.
[25] Nicolas G, Bennoun M, Devaux I, Beaumont C, Grandchamp B, Kahn A, *et al*. Lack of hepcidin gene expression and severe tissue iron overload in upstream stimulatory factor 2 (USF2) knockout mice. Proc Natl Acad Sci U S A 2001;98(15):8780–8785. doi:10.1073/pnas.151179498.
[26] Varghese J, Varghese James J, Karthikeyan M, Rasalkar K, Raghavan R, Sukumaran A, *et al*. Iron homeostasis is dysregulated, but the iron-hepcidin axis is functional, in chronic liver disease. J Trace Elem Med Biol 2020;58:126442. doi:10.1016/j.jtemb.2019.126442.
[27] Costa-Matos L, Batista P, Monteiro N, Simões M, Egas C, Pereira J, *et al*. Liver hepcidin mRNA expression is inappropriately low in alcoholic patients compared with healthy controls. Eur J Gastroenterol Hepatol 2012;24(10):1158–1165. doi:10.1097/MEG.0b013e328355cfd0.
[28] Ryan JD, Altamura S, Devitt E, Mullins S, Lawless MW, Muckenthaler MU, *et al*. Pegylated interferon-α induced hypoferremia is associated with the immediate response to treatment in hepatitis C. Hepatology 2012;56(2):492–500. doi:10.1002/hep.25666.
[29] Armitage AE, Stacey AR, Giannoulatou E, Marshall E, Sturges P, Chatha K, *et al*. Distinct patterns of hepcidin and iron regulation during HIV-1, HBV, and HCV infections. Proc Natl Acad Sci U S A 2014;111(33):12187–12192. doi:10.1073/pnas.1402351111.
[30] Lin D, Ding J, Liu JY, He YF, Dai Z, Chen CZ, *et al*. Decreased serum hepcidin concentration correlates with brain iron deposition in patients with HBV-related cirrhosis. PLoS One 2013;8(6):e65551. doi:10.1371/journal.pone.0065551.
[31] Vela D. Low hepcidin in liver fibrosis and cirrhosis; a tale of progressive disorder and a case for a new biochemical marker. Mol Med 2018;24(1):5. doi:10.1186/s10020-018-0008-7.
[32] Wang J, Dong A, Liu G, Anderson GJ, Hu TY, Shi J, *et al*. Correlation of serum hepcidin levels with disease progression in hepatitis B virus-related disease assessed by nanopore film based assay. Sci Rep 2016;6:34252. doi:10.1038/srep34252.
[33] Çam H, Yılmaz N. Serum hepcidin levels are related to serum markers for iron metabolism and fibrosis stage in patients with chronic hepatitis B: A cross-sectional study. Arab J Gastroenterol 2020;21(2):85–90. doi:10.1016/j.ajg.2020.04.013.
[34] Lyberopoulou A, Chachami G, Gatselis NK, Kyratzopoulou E, Saitis A, Gabeta S, *et al*. Low Serum Hepcidin in Patients with Autoimmune Liver Diseases. PLoS One 2015;10(8):e0135486. doi:10.1371/journal.pone.0135486.
[35] Sumida Y, Yoneda M. Current and future pharmacological therapies for NAFLD/NASH. J Gastroenterol 2018;53(3):362–376. doi:10.1007/s00535-017-1415-1.
[36] Miura K, Yang L, van Rooijen N, Ohnishi H, Seki E. Hepatic recruitment of macrophages promotes nonalcoholic steatohepatitis through CCR2. Am J Phys-

iol Gastrointest Liver Physiol 2012;302(11):G1310–G1321. doi:10.1152/ajpgi.00365.2011.
[37] Tacke F. Targeting hepatic macrophages to treat liver diseases. J Hepatol 2017;66(6):1300–1312. doi:10.1016/j.jhep.2017.02.026.
[38] Camaschella C, Nai A, Silvestri L. Iron metabolism and iron disorders revisited in the hepcidin era. Haematologica 2020;105(2):260–272. doi:10.3324/haematol.2019.232124.
[39] Zlatanova I, Pinto C, Bonnin P, Mathieu JRR, Bakker W, Vilar J, *et al*. Iron Regulator Hepcidin Impairs Macrophage-Dependent Cardiac Repair After Injury. Circulation 2019;139(12):1530–1547. doi:10.1161/CIRCULATIONAHA.118.034545.
[40] Liu E, Li Z, Zhang Y, Chen K. Hepcidin Induces M1 Macrophage Polarization in Monocytes or THP-1 Derived Macrophages. Iran J Immunol 2019;16(3):190–199. doi:10.22034/IJI.2019.80270.
[41] Gan ZS, Wang QQ, Li JH, Wang XL, Wang YZ, Du HH. Iron Reduces M1 Macrophage Polarization in RAW264.7 Macrophages Associated with Inhibition of STAT1. Mediators Inflamm 2017;2017:8570818. doi:10.1155/2017/8570818.
[42] Han CY, Koo JH, Kim SH, Gardenghi S, Rivella S, Strnad P, *et al*. Hepcidin inhibits Smad3 phosphorylation in hepatic stellate cells by impeding ferroportin-mediated regulation of Akt. Nat Commun 2016;7:13817. doi:10.1038/ncomms13817.
[43] Détivaud L, Nemeth E, Boudjema K, Turlin B, Troadec MB, Leroyer P, *et al*. Hepcidin levels in humans are correlated with hepatic iron stores, Hb levels, and hepatic function. Blood 2005;106(2):746–748. doi:10.1182/blood-2004-12-4855.
[44] Lunova M, Goehring C, Kuscuoglu D, Mueller K, Chen Y, Walther P, *et al*. Hepcidin knockout mice fed with iron-rich diet develop chronic liver injury and liver fibrosis due to lysosomal iron overload. J Hepatol 2014;61(3):633–641. doi:10.1016/j.jhep.2014.04.034.
[45] Lu S, Bennett RG, Kharbanda KK, Harrison-Findik DD. Lack of hepcidin expression attenuates steatosis and causes fibrosis in the liver. World J Hepatol 2016;8(4):211–225. doi:10.4254/wjh.v8.i4.211.
[46] Park PH, Sanz-Garcia C, Nagy LE. Adiponectin as an anti-fibrotic and anti-inflammatory adipokine in the liver. Curr Pathobiol Rep 2015;3(4):243–252. doi:10.1007/s40139-015-0094-y.
[47] Xu H, Zhao Q, Song N, Yan Z, Lin R, Wu S, *et al*. AdipoR1/AdipoR2 dual agonist recovers nonalcoholic steatohepatitis and related fibrosis via endoplasmic reticulum-mitochondria axis. Nat Commun 2020;11(1):5807. doi:10.1038/s41467-020-19668-y.